2016 IEEE/RSJ International Conference on Intelligent Robots and Systems (IROS)
Daejeon Convention Center
October 9-14, 2016, Daejeon, Korea

Keyframe based Large-Scale Indoor Localisation using Geomagnetic Field and Motion Pattern

Sen Wang, Hongkai Wen, Ronald Clark and Niki Trigoni

***Abstract*— This paper studies indoor localisation problem by using low-cost and pervasive sensors. Most of existing indoor localisation algorithms rely on camera, laser scanner, floor plan or other pre-installed infrastructure to achieve sub-meter or sub-centimetre localisation accuracy. However, in some circumstances these required devices or information may be unavailable or too expensive in terms of cost or deployment. This paper presents a novel keyframe based Pose Graph Simultaneous Localisation and Mapping (SLAM) method, which correlates ambient geomagnetic field with motion pattern and employs low-cost sensors commonly equipped in mobile devices, to provide positioning in both unknown and known environments. Extensive experiments are conducted in large-scale indoor environments to verify that the proposed method can achieve high localisation accuracy similar to state-of-the-arts, such as vision based Google Project Tango.**

I. Introduction

Localising humans in Global Positioning System (GPS) denied indoor environments by using low-cost and pervasive sensors remains a challenging problem. When many practical requirements, such as reducing system cost and protecting privacy, are considered, it becomes more difficult.

Some conventional solutions rely on dedicated infrastructure or powerful sensors, such as laser scanner, to conduct indoor localisation. However, they could be expensive in terms of system setting up or device cost. Although floor plan and opportunistic signals, e.g., radio and WiFi, can be utilised to realise indoor localisation in an inexpensive manner, they are subject to availability and reliability. Leveraging ubiquitous information and low-cost sensors to achieve accurate ego-motion is increasingly demanded.

Recently, vision based method has attracted considerable interest [1], [2] as cameras have been available in most of mobile devices. It is a promising technique which can perform high-precision localisation and mapping. However, in some scenarios cameras are not allowed due to security and privacy concerns. Unlike outdoor applications, indoor localisation needs to take privacy into particular consideration. For example, "No Photography" sign can be usually found in buildings. Besides, it may be uncomfortable or unacceptable to consistently face a camera around. In addition, vision based techniques tend to be computationally expensive, consuming much energy.

Geomagnetic field which has noticeable signatures for different indoor areas can be a viable alternative because it has been known that animals use it for navigation [3]. As an ambient signal, geomagnetic field has several special characteristics in indoor environments, which make it suitable for localisation. It presents ubiquitously with significant anomalies owing to various distortion sources, such as electric equipment and rebar in building structures. Meanwhile, the anomalies are reasonably stable in a long period of time. The fluctuation in the geomagnetic field is also easy to measure by normal mobile devices.

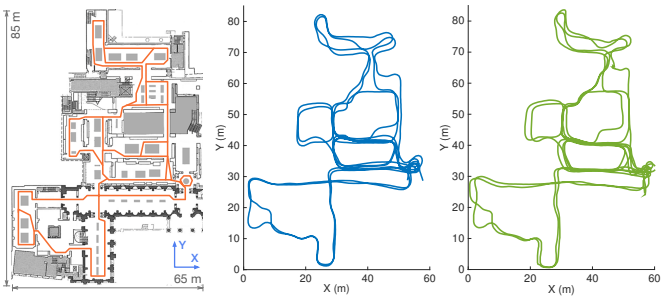

(a) Floor plan and path. (b) Proposed method. (c) Google Tango.

Fig. 1. (a) Floor plan of a museum (about $5000m^2$ in size) superimposed with trajectory. Note the trajectory only shows an approximate path rather than ground truth and floor plans throughout the whole paper are for visualisation purpose only. (b) Localisation result of proposed method after $1.2km$ walking. (c) Corresponding localisation result of Google Tango.

In order to benefit from a geomagnetic field, there are some challenges to tackle [4]. Since the anomaly of an indoor geomagnetic field is highly non-linear and seriously coupled with surroundings, it is extremely difficult to model or predict it accurately. This means a prior map of a geomagnetic field is unavailable. Therefore, fingerprinting is popular to obtain it before localisation. Collecting fingerprints, however, is labour-intensive and time-consuming in large-scale spaces and is inapplicable in unknown environments. Moreover, the anomalies of a geomagnetic field are only discriminative to some extent, i.e., a unique location signature may not be guaranteed. In fact, a single geomagnetic measurement is not informative enough to provide position estimation.

In this paper, a novel keyframe based approach is proposed to achieve accurate and reliable ego-motion estimation by making full use of geomagnetic field, motion pattern and low-cost sensors. It is applicable to devices which contain accelerometer, gyroscope and magnetometer, e.g., a normal mobile phone. The main contribution is threefold: 1) A keyframe based loop closure detection which correlates geomagnetic measurements with motion pattern is developed to build reliable front-end for graph optimisation. Since the keyframes are generated in local coordinate systems, it is

The authors are with Department of Computer Science, University of Oxford, Oxford OX1 3QD, United Kingdom {firstname.lastname}@cs.ox.ac.uk

efficient for large-scale environments. 2) A Graph Simultaneous Localisation and Mapping (SLAM) based algorithm is proposed to simultaneously localise devices and generate geomagnetic map with small human effort in unknown environments. A user can conduct this by simply holding a mobile device and walking. 3) Motion pattern is incorporated with a prior geomagnetic map of a known environment for real-time localisation in the framework of Bayesian filtering. It eliminates the dependence on highly non-linear and complicated physical models of indoor geomagnetic fields or fine-grained geomagnetic maps for localisation in large spaces.

The rest of this paper is organised as follows. Section II reviews related work. The proposed algorithms in unknown and known environments are provided in Section III and IV, respectively. Section V presents experimental results. Finally, conclusion is drawn in Section VI.

II. Related Work

Recently, geomagnetic field based indoor localisation has attracted significant interest in both academia and industry. Related work is reviewed in this section, discussing differences between the proposed method and existing ones.

In order to perform localisation, some methods build a geomagnetic map in advance by using fingerprinting [4]–[9], etc. Then, matching of geomagnetic fields [4]–[8], [10] or Bayesian filtering [9], [11]–[13] is adopted to localise a robot or person with respect to the built geomagnetic map. Specifically, in [5] landmarks, such as rooms and corridors, are recognised by matching geomagnetic fields against a geomagnetic map generated from fingerprinting. Euclidean distance based Least Mean Square is used in [4] to check similarity between magnetic measurements and map, deriving positions with respect to the known map. However, Euclidean distance metric is seriously degraded by signal contraction and expansion. Therefore, Dynamic Time Warping (DTW) is employed in [7], [8] to classify magnetic signatures which are not temporally well aligned. Similarly, DTW is used in [10] to match magnetic sequences against previously recorded ones. In order to consider motion model, [9] fuses dead-reckoning information from robots and humans with geomagnetic maps by using Monte Carlo Localisation (MCL). However, the algorithm is developed for one-dimensional localisation and the map is built based on positions solely from dead-reckoning, which is prone to drift. Motion capture system is utilised in [11] to provide accurate poses for creating high-precision geomagnetic map, which is adopted for localisation of legged and non-legged locomotion based on MCL. The system, however, is confined in a space where motion capture system covers and relies on two foot-mounted Inertial Measurement Unit (IMU) sensors. [12] also proposes MCL based on a magnetic map that is built by a robot using Gaussian process (GP) although a laser based robot localisation is required to estimate poses when mapping the magnetic field. In [13], MCL based method does not require special hardware but a floor plan of an environment is necessary to build a geomagnetic map.

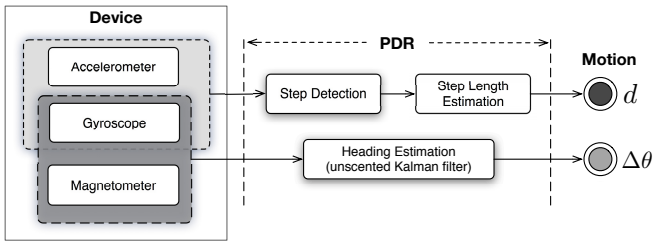

Fig. 2. PDR based estimation on displacement and heading change.

The previous work does not accurately localise platforms that measure the geomagnetic field or acquires locations from additional devices, such as motion capture system and laser scanner. Moreover, it is not applicable to unknown environments. In order to overcome these, SLAM based approaches are developed [14], [15]. In [14], MCL based SLAM is proposed for robot localisation by modelling the geomagnetic field using GP. However, due to limitations of GP for large-scale environments, experiments are conducted in rather small areas (about $100m^2$ in size). In contrast, MCL based SLAM algorithm in [15] can be applied for large-scale indoor environments by using IMU and geomagnetic field. Although the proposed approach is superior, IMU sensor has to be mounted on foot.

Graph SLAM is recently introduced for geomagnetic field based localisation [16], [17]. In [16], sequences of geomagnetic measurements are matched by Euclidean distance based loop closure detection for robot localisation. Since Euclidean distance metric does not work well in the present of misalignment or handle sequences with different sizes, it is difficult to detect loop closure with varying speeds. Moreover, there is no particular consideration on how to reduce the number of false-positive closures. [17] uses DTW for sequence matching and checks segment topology based on variances of sequences' coordinates. However, a WiFi and Bluetooth signal map is employed for localisation rather than geomagnetic maps. Meanwhile, loop closure detection is limited in $10m$ distance to reduce false-positives. This could be a strong hypothesis which assumes small drift of dead-reckoning, making loop closures undetected in large-scale environments.

III. Keyframe based Graph SLAM in Unknown Environments

In this section, keyframe based Graph SLAM by using geomagnetic field and motion pattern is proposed to achieve localisation and build geomagnetic map simultaneously in unknown environments. It is composed of dead-reckoning, keyframe based front-end construction (keyframe generation and loop closure detection) and graph optimisation.

A. Dead-Reckoning

Dead-reckoning provides motion perdition without relying on exteroceptive devices. Robot localisation usually performs dead-reckoning by using odometry which is not available for mobile devices. In this work, Pedestrian Dead Reckoning

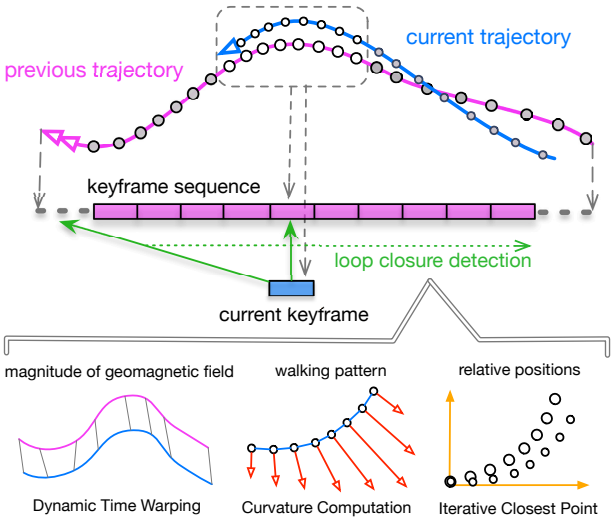

Fig. 3. Keyframe generation and loop closure detection.

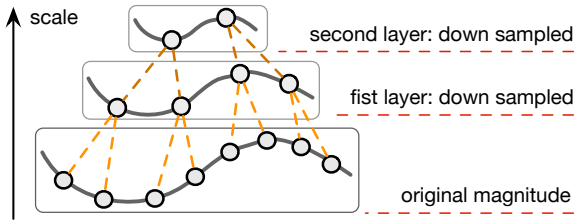

Fig. 4. Pyramid representation of multi-scaled magnitudes of magnetic field. Measurements of magnitudes are down-sampled by a factor of 2 for each layer.

(PDR) [18], which uses an accelerometer, a gyroscope and a magnetometer to estimate displacement and heading change with respect to a previous pose, is adopted as a solution to dead-reckoning. As shown in Fig. 2, it mainly consists of step detection, step length estimation and heading estimation. A zero crossing detector with linear stride length model is used to estimate step length, while relative heading is computed by fusing readings from a magnetometer and a gyroscope in the framework of unscented Kalman filter. For each step, the PDR derives motion $\hat{\mathbf{u}}_k = [d_k, \Delta\theta_k]^T$ where d_k and $\Delta\theta_k$ are displacement and heading change of step k, respectively, with respect to last pose.

PDR can calculate movement of each step with a relatively small error. However, as one kind of dead-reckoning techniques, it also suffers from significant drift over time, especially compared with foot-mounted PDR. For instance, Fig. 15(a) shows a drifted PDR trajectory. In order to amend this, Graph SLAM using geomagnetic field and motion pattern is proposed.

B. Keyframe Generation

Since it is known that a single observation is not informative enough to distinguish ambiguities of a geomagnetic field [10], [16], [17], the main idea of our keyframe based method is to incorporate geomagnetic measurements with motion, increasing information dimension and then realising reliable loop closure detection. To this end, a keyframe is described by features extracted from both geomagnetic field and motion pattern in several consecutive steps, see Fig. 3.

Keyframes are consistently generated as travelling in the environment. For each keyframe, it is composed of the following three parts:

1) Multi-Scaled Magnitudes of Geomagnetic Field. Although the maximum sampling rate of a magnetometer is around several hundreds Hertz, to reduce computation and increase resilience to noise, magnitudes of geomagnetic field are gathered together in a step-specific manner, i.e., for a step there is only one magnetic reading averaged over measurements of the step. Then, a coarse-to-fine representation is introduced. Specifically, as shown in Fig. 4, the original sequence of magnitudes of a geomagnetic field is down-sampled to several new layers by a factor of 2. This multi-scaling approach is widely used in the computer vision community to increase efficiency and mitigate influence of noise. We use the magnitude rather than three-axis readings because the magnitude is not affected by device orientation and it is difficult to consistently track device orientation in 3D by only using an IMU and a magnetometer.
2) Walking Pattern. Curvature of each step with respect to last one is computed. A set of curvatures is used to determine a walking pattern in a keyframe, such as turning direction and angle, and optionally reduce the number of keyframes.
3) Relative Positions. In order to alleviate the drift problem of PDR, the motion trajectory in a keyframe is represented as relative positions in a local coordinate system. Taking the initial pose of the trajectory in a keyframe as the origin of a coordinate frame and transforming subsequent steps in this keyframe to this coordinate frame produce a set of poses defined in the local coordinate system.

Keyframes can be created for the whole trajectory or when the motion pattern satisfies some requirements. For example, since walking straight gives limited information on movement, producing keyframes only around turning points dramatically reduces the number of keyframes, enhancing efficiency of keyframe search during loop closure detection.

C. Loop Closure Detection

Along with the keyframe generation, loop closure of keyframes is detected to build a front-end pose graph for Graph SLAM. A current keyframe is maintained to conduct keyframe based similarity search. As shown in Fig. 3, there are mainly three parts in the loop closure detection.

1) Magnitudes of Geomagnetic Field: DTW which measures distance between two temporal signals by using dynamic programming [19] is employed for similarity check of magnitudes of a geomagnetic field. This is because DTW distance is better than Euclidean distance if two sequences have different sizes or misalignment in terms of phase, see Euclidean matching of two sequences of magnitudes of a

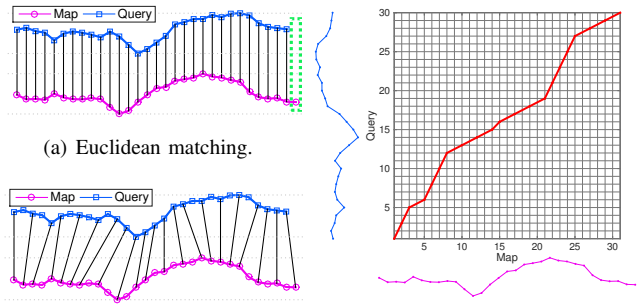

(a) Euclidean matching.

(b) DTW matching.

(c) DTW warping path.

Fig. 5. Euclidean and DTW alignments of two sequences of magnitudes of a geomagnetic field. Euclidean distance metric cannot handle misalignment or series with different sizes (missing matching marked in (a)).

geomagnetic field in Fig. 5(a) and its DTW counterpart in Fig. 5(b). Therefore, it realises more robust similarity check in terms of different walking speed and pattern. Fig. 5(c) presents corresponding warping matrix and optimal warping path to align the two sequences. The DTW based matching is performed in a top-down manner for each layer of the multi-scaled magnitudes. The pyramid representation of magnitudes in Section III-B achieves efficient matching and offers more resilience to noise.

2) Walking Pattern: Since magnitudes of a geomagnetic field are only one-dimensional time-series signals, they are not informative enough to distinguish many keyframes in large environments, especially when each keyframe is only built by few steps. Therefore, it is necessary to incorporate other information. Walking patterns, such as turning direction and angles, are adopted to correlate with geomagnetic measurements, which indirectly increases the dimension of the data. Because turns are one of the most salient features during human walking, keyframes generated around turns are compared in terms of turning direction and curvature. DTW based curvature matching is employed to tackle the problem of different turning speeds. Meanwhile, keyframes obtained from straight walking are tested with an extra requirement on variance of magnitudes of a geomagnetic field, ensuring more reliable matching. This is because we usually walk straight in indoor environments and it is less informative than turning. Note that since the curvature is computed between two consecutive steps, the walking pattern is accurate although PDR drifts over time in global coordinate systems.

3) Relative Positions: The set of relative positions in a keyframe defines a trajectory in a local coordinate system. As shown in Fig. 6, two sets of relative positions in their local coordinate systems could have rather big Euclidean distance without rotation. In order to mitigate this effect, Iterative Closest Point (ICP) which considers translation and orientation without scaling is employed to check similarity of the trajectories in different keyframes, see the matching after ICP in Fig. 6. Since there are only several positions in a keyframe and rotation between trajectories in two candidate keyframes tends to be small, the ICP is very efficient.

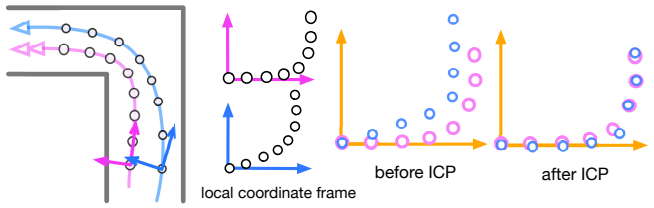

Fig. 6. ICP Matching of relative positions in two keyframes which have different local coordinate frames.

D. Graph Optimisation

If a loop closure is detected between two keyframes, their consecutive poses are correspondingly connected. Then, a pose graph is produced after the loop closure detection. However, there may be some false-positives in large-scale environments, particularly for geomagnetic field based methods which have limited information compared to vision based ones. Therefore, a robust graph optimisation is necessary. In this work, Vertigo [20] is employed as the back-end of the pose Graph SLAM.

IV. Localisation within Prior Geomagnetic Maps

This section describes an approach to utilising a prior geomagnetic map and motion pattern for localisation in the framework of Bayesian filtering. Once a geomagnetic map of an unknown environment is built by the algorithm in the previous section, localisation can be realised in real-time based on it. This not only reduces computation costs without using the Graph SLAM any more, but also enables the system to work in a many-to-many way, i.e., users who are new to an environment can benefit from a map built and shared by others. Since the geomagnetic map is solely composed of magnitudes of a geomagnetic field at different locations, its size is very small (the size of our map of the $5000m^2$ museum is about 100 Kilobytes), which makes the geomagnetic field based method suitable for resource-constrained devices. This is different from image sequences or point cloud maps adopted by techniques relying on vision.

Because indoor geomagnetic fields are highly non-linear and location-specific, it is difficult to model them. Therefore, based on the architecture of the keyframe based method in last section, a Kalman Filter (KF) based algorithm is proposed to fuse PDR with measurements incorporating geomagnetic maps and motion information. Although other kinds of Bayesian estimation techniques, such as particle filters, can be applied, KF could be more efficient, in particular for mobile devices.

A. Prediction

The PDR in Section III-A is introduced as prediction. Then, the process model is

$$\mathbf{x}_k = f(\mathbf{x}_{k-1}, \mathbf{u}_k, \mathbf{w}_k) \tag{1}$$

where $\mathbf{x}_k$ is the pose at time k, $\mathbf{u}_k$ is the motion between time $k-1$ and k, and $\mathbf{w}_k \sim \mathcal{N}(0, \mathbf{Q}_k)$ is an additive Gaussian noise on this dead-reckoning.

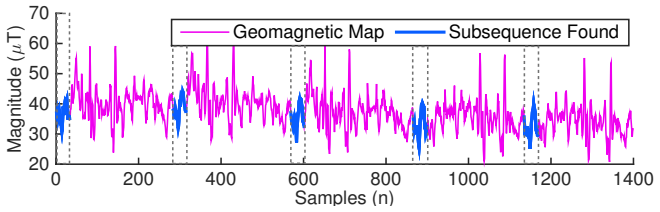

Fig. 7. DTW based subsequence search. There could be several matched candidates.

B. Update based on Geomagnetic Map and Motion

Since the PDR drifts over time, the predicted state needs to be corrected. Instead of directly taking geomagnetic observations as measurements, they are correlated with motion information to obtain pose measurements on the available geomagnetic map according to the keyframe based method in Section III. This allows us to get rid of highly non-linear and complicated physical models of indoor geomagnetic fields or fine-grained geomagnetic maps in large spaces [21]. Specifically, last several PDR steps and observations of magnitudes of a geomagnetic field are combined together to produce a keyframe to be searched. Firstly, a DTW based subsequence search of magnitudes against the geomagnetic map is conducted to find potential matches. In case the size of the geomagnetic map is huge, the search is limited to $\pm 3\sigma$ confidence interval of $\mathbf{x}_k$ to reduce computational cost. The DTW based subsequence search could find a few candidates matched in the geomagnetic map, as shown in Fig. 7. Secondly, the found candidates are checked according to the criteria of the walking pattern and the relative positions in Section III. It could be possible to still have several candidates left. Thirdly, in order to find the true-positive matches, these candidates are clustered into some groups in terms of their poses on the geomagnetic map. The groups are ranked according to the number of the candidates, the DTW distances and the ICP distances. The candidates in the best matched group are selected to generate a pose measurement for KF. Therefore, the measurement model at time t is

$$\mathbf{z}_k = h(\mathbf{x}_k, \mathbf{v}_k) \tag{2}$$

where $\mathbf{z}_k$ is the measured pose on the geomagnetic map and $\mathbf{v}_k \sim \mathcal{N}(0, \mathbf{R}_k)$ is a Gaussian noise. Due to the simplicity of the KF, the details on how to update the state and the covariance are omitted here.

V. Experimental Results

The proposed method is tested in two indoor environments to evaluate its performance. One is an office building (about $1100m^2$ in size), while the other is a museum (about $5000m^2$ in size). Since both of the scenarios are public and large-scale, it is difficult to obtain accurate ground truth. Therefore, a Google Project Tango device [22], which is a state-of-the-art vision aided inertial navigation system providing accurate positioning (about $0.1\% - 0.5\%$ drift of travelling distance), is attached onto our mobile device to evaluate the proposed algorithm. Note that the Tango is introduced for evaluation purposes only, and we are not trying to compete against it. This is because the proposed method is a SLAM system, while the Tango is an odometry technique which uses camera and is capable of estimating motion in 6 Degree-of-Freedom. A Google Nexus 5 mobile phone is used in our experiments.

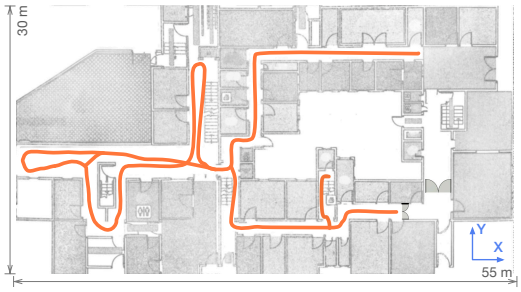

(a) Floor plan and path.

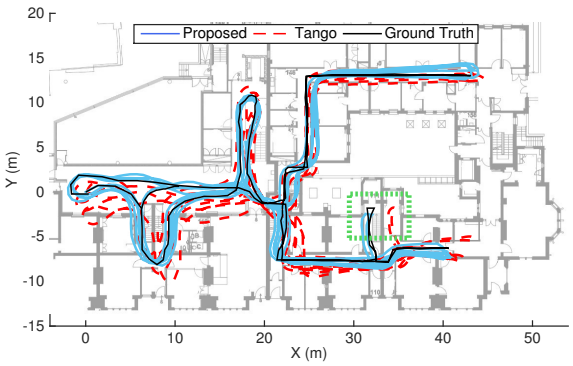

(b) Pseudo ground truth and results of proposed method and Tango.

Fig. 8. Localisation in the office building. (a) Floor plan of an office building superimposed with trajectory. Note the trajectory only shows an approximate path rather than ground truth. (b) Pseudo ground truth and localisation results.

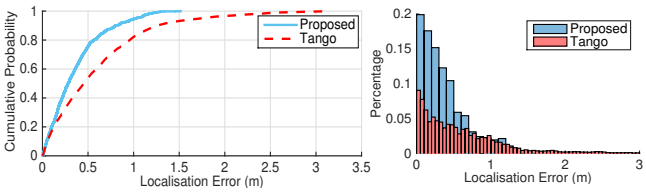

(a) Distribution of errors. (b) Histogram of errors.

Fig. 9. Distribution and histogram of the localisation errors in the office building.

A. Results in Unknown Environments

The floor plan of the office building and the walking trajectory are shown in Fig. 8(a). As mentioned before, the trajectory only shows an approximate path rather than ground truth. A person walks about $0.75km$ in the building, holding the mobile phone and the Tango at the same time. Since the Tango drifts slightly fast in this indoor environment, it is not very meaningful to directly compare the localisation results against its. Therefore, in order to evaluate the performance quantitatively, a pseudo ground truth is manually marked on the floor plan and further interpolated into fine grids. Although there may be errors of the manually selected points,

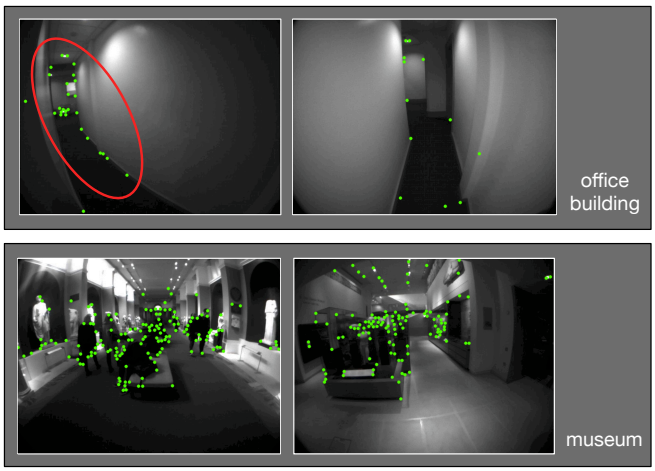

Fig. 10. Features extracted from images of wide-angle camera of Google Tango. In some challenging indoor environments, such as corridors in the office building, most of features gather around texture objects or the number of features is limited. Vision based methods benefit from open space areas. In contrast, the geomagnetic field based method is not affected.

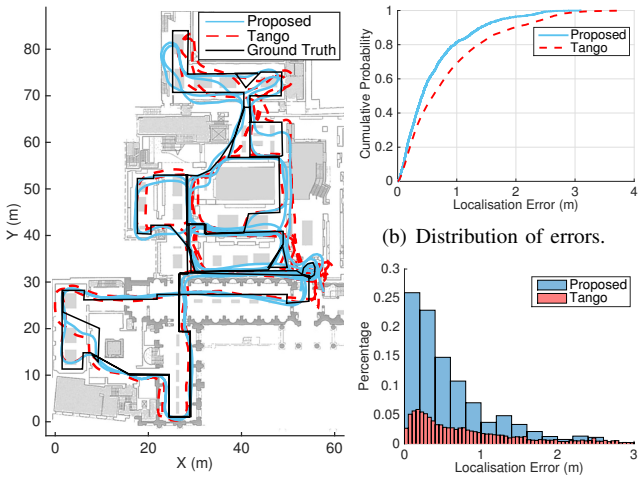

(a) Ground truth and localisation results. (b) Distribution of errors. (c) Histogram of errors.

Fig. 11. Localisation in the museum. (a) Pseudo ground truth and localisation results of proposed method and Tango. (b) Cumulative distribution of the localisation errors. (c) Histogram of the localisation errors.

scale problem of the floor plan, etc., this ground truth can still reflect the performance to some extent. The pseudo ground truth and the localisation results of the proposed method and the Tango are given in Fig. 8(b). It can be seen that the proposed method can achieve better localisation accuracy than the Tango. For example, for the part marked by dashed lines, the positions estimated by the proposed method are close to the ground truth, while these of the Tango are located in a wrong room.

Fig. 9 presents the distribution and the histogram of the localisation errors in the office building. Specifically, as shown in Fig. 9(a), 80% of the positions estimated by the proposed method are within $0.5m$ errors, while it is $1m$ for the Tango. The histograms of the two methods in Fig. 9(b) also describes the proposed method can provide reliable localisation results within high accuracy.

Since the office building has some narrow spaces with texture-less surroundings, such as white walls shown in Fig. 10, it is sometimes challenging for vision based techniques to work well. This should be also one of important reasons why the Tango drifts slightly fast. Meanwhile, it suggests that our proposed method could be an appealing alternative or additional auxiliary system for vision based approaches.

In order to improve the Tango's performance for further evaluation, a public museum which has many open spaces and texture-rich objects is adopted. The floor plan and the estimated trajectories after about $1.2km$ walking are given in Fig. 1. Fig. 11(a) shows the corresponding pseudo ground truth and localisation results, which suggest the similar performance as in the office building. For this large-scale environment, 80% of the errors of the proposed method are less than $1m$, see the distribution of errors in Fig. 11(b). This slightly outperforms the results of the Tango. Fig. 11(c) demonstrate the percentages of the localisation errors in the form of histogram.

The mean, maximum and minimum of root mean squared errors of the proposed method and the Tango in the two scenarios are given in TABLE I. For the proposed method, the mean errors are $0.3676m$ and $0.6014m$ in the office building and the museum, respectively. In general, the performance of the proposed method is better than that of the Tango, which further verifies that the geomagnetic field based approach is capable of achieving high localisation accuracy. Since the proposed method only employs the ambient geomagnetic field and the low-cost and pervasive sensors, there are some advantages when it is applied in practice.

TABLE I
ERRORS (METER) OF THE TWO SCENARIOS

	Office		Museum	
	Proposed	Tango	Proposed	Tango
Mean	**0.3676**	0.6239	**0.6014**	0.8273
Maximum	**1.5168**	3.4395	**3.0938**	3.8292
Minimum	0.0022	**0.0003**	0.0078	**0.0012**

B. Loop Closure Detection

The loop closure detection is discussed to show why incorporating geomagnetic field with motion pattern can significantly improve it. Fig. 12(a) presents a false-positive loop closure of two keyframes detected by only using geomagnetic measurements. According to Fig. 12(b), their magnitudes of the geomagnetic field are similar. However, when the motion patterns are taken into consideration, the false-positive loop closure can be easily rejected, see big differences presented in their curvatures and ICP results in Fig. 12(c) and Fig. 12(d), respectively.

Precision-recall curve is shown in Fig. 13. Since empirical curve reduces accuracy with a small set of samples, an alpha-binormal model based precision-recall curve [23] is also given in Fig. 13(b). It can be seen that the precision is considerably increased once introducing motion pattern into loop closure detection. This is coherent to the example in

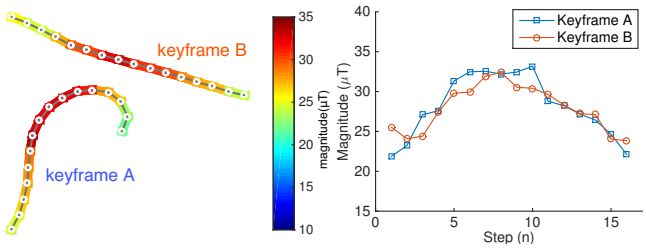

(a) Two keyframes. (b) Magnitudes of geomagnetic field.

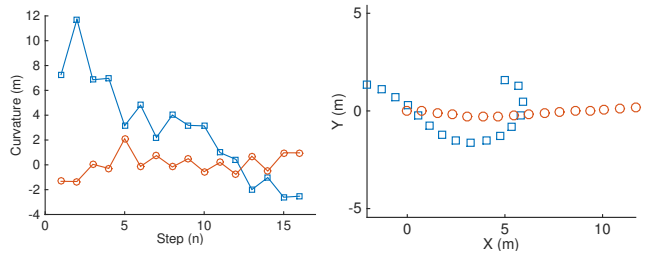

(c) Curvature. (d) ICP.

Fig. 12. False-positive loop closure detected by only using geomagnetic measurements can be rejected when considering motion pattern.

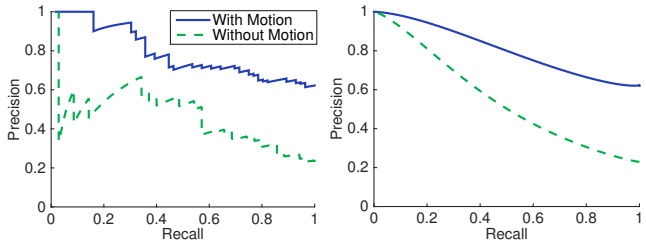

(a) Empirical curve. (b) Model-based curve.

Fig. 13. Precision-recall curve.

Fig. 12. Since in this work the loop closure is detected across the whole map rather than limited in a certain small space as in [17], it tends to suffer from more false-positives. The motion pattern is particularly useful for this. In fact, without correlating motion information, the number of false-positive loop closures dramatically grows.

C. Results in Known Environments

Once a map of a geomagnetic field is built by the proposed algorithm for unknown environments, the localisation can be performed in real-time based on it. The geomagnetic map of the office building produced by the experiment in Section V-A is given in Fig. 14, whose colour represents the different magnitudes of the geomagnetic field. It can be seen that the anomalies of the geomagnetic field are location-specific. The consistency of the map also verifies the high localisation accuracy of the proposed method for unknown environments.

In order to test the proposed method in known environments in Section IV, a person walks randomly with a mobile phone. Fig. 15(a) and Fig. 15(b) present the PDR and the localisation results, respectively. While the PDR drifts significantly, the localisation results of the proposed method consistently match the floor plan. For instance, as shown in the enlargement, all of the trajectories are located

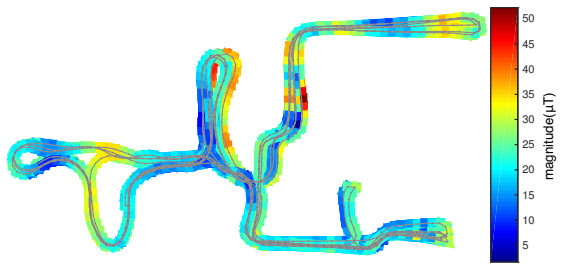

Fig. 14. Geomagnetic map of the office building built by our algorithm for unknown environments. The colour bar indicates the magnitudes of the geomagnetic field (μT).

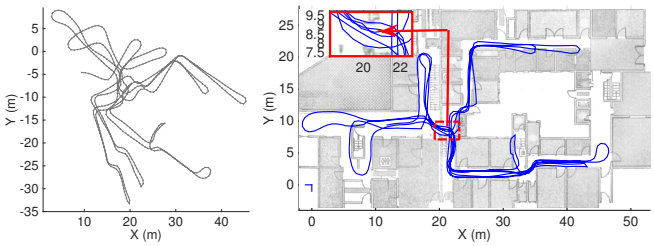

(a) PDR of random walk. (b) Localisation results.

Fig. 15. Localisation in the office building based on the geomagnetic map in Fig. 14. (a) PDR of a random walk. (b) Corresponding localisation results.

in the doorway which is about $1m$ wide. Note that as aforementioned the floor plan is used only for visualisation purpose rather than localisation.

The geomagnetic map and the localisation results of the museum are provided in Fig. 16. Based on the geomagnetic map in Fig. 16(a), the proposed method can achieve high localisation accuracy which is similar or better than the Tango's, see Fig. 16(b) and two enlarged parts in it. Moreover, the proposed method is applicable to unmapped areas, such as the shaded portion in Fig. 16(b). Fig. 16(c) shows $\pm 3\sigma$ confidence intervals of this test. It can be seen that the uncertainties are all bounded over time, which indicates that the pose measurements from the geomagnetic map and the motion pattern are reliable. It is worth mentioning that there are about 2 months gap between building the geomagnetic map and conducting the localisation, which means the geomagnetic field is temporally stable for a while and our proposed method is efficient to handle the variations.

VI. Conclusions

This paper presents an indoor localisation system for both unknown and known environments based on geomagnetic field and motion pattern. A keyframe based Graph SLAM approach is proposed to simultaneously achieve accurate positioning and generate geomagnetic maps in unknown environments. Based on a prior map and motion pattern, localisation can be performed by Bayesian filtering in real-time. The effectiveness of the proposed system is validated by extensive experiments in two large-scale scenarios. The geomagnetic field is ubiquitous and the sensors required by the system are low-cost and pervasive. Therefore, the system could be auxiliary for others. Meanwhile, it is easy to use by

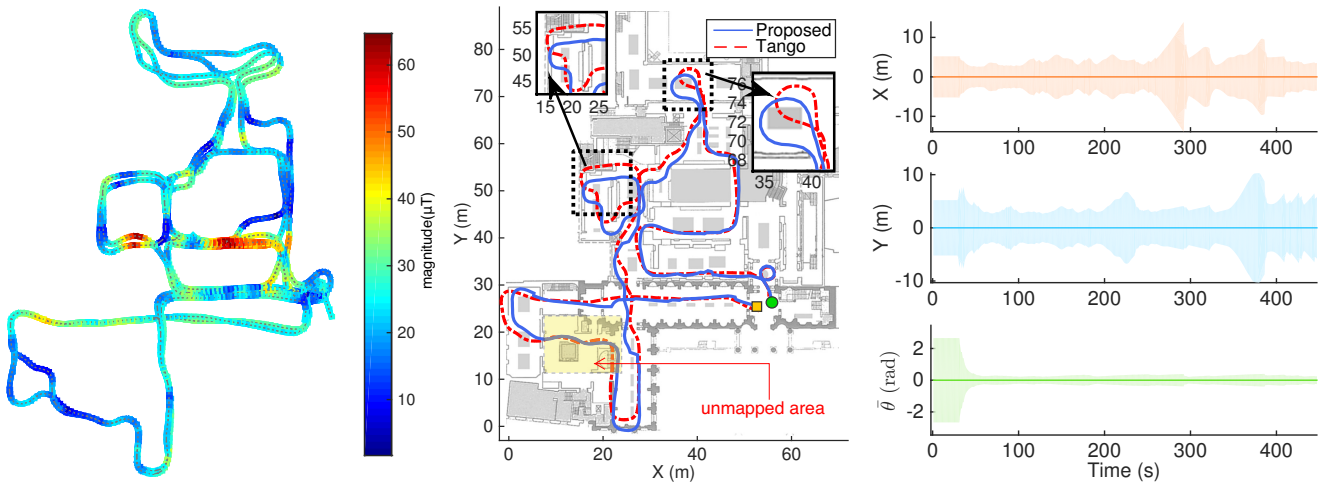

(a) Geomagnetic map of the museum. (b) Localisation results. (c) 3σ confidence intervals.

Fig. 16. Localisation in the museum based on a prior geomagnetic map. (a) Geomagnetic map of the museum built by our algorithm for unknown environments. (b) Localisation results of a random walk. Starting and ending points are marked as a (green) circle and a (orange) square, respectively. (c) 3σ confidence intervals of the localisation in the museum.

simply walking around with a mobile device. Anyone having a mobile phone can benefit from and contribute to the system by navigating in unknown environments and building and sharing a geomagnetic map.

Although the proposed technique works well in constrained indoor spaces, like corridor and small rooms, it tends to fail in large open spaces if the trajectories are not similar. Our future work will focus on how to solve this.

ACKNOWLEDGMENT

This work has been supported by EPSRC Program Grant "Mobile Robotics: Enabling a Pervasive Technology of the Future (GoW EP/M019918/1)".

REFERENCES

[1] S. Ito, F. Endres, M. Kuderer, G. Diego Tipaldi, C. Stachniss, and W. Burgard, "W-rgb-d: floor-plan-based indoor global localization using a depth camera and wifi," in *Proc. IEEE Int. Conf. Robot. Autom.* IEEE, 2014, pp. 417–422.

[2] W. Winterhalter, F. Fleckenstein, B. Steder, L. Spinello, and W. Burgard, "Accurate indoor localization for RGB-D smartphones and tablets given 2D floor plans," in *Proc. IEEE/RSJ Int. Conf. Intell. Robots Syst.* IEEE, 2015, pp. 3138–3143.

[3] L. C. Boles and K. J. Lohmann, "True navigation and magnetic maps in spiny lobsters," *Nature*, vol. 421, no. 6918, pp. 60–63, 2003.

[4] J. Chung, M. Donahoe, C. Schmandt, I.-J. Kim, P. Razavai, and M. Wiseman, "Indoor location sensing using geo-magnetism," in *International Conference on Mobile Systems, Applications, and Services*. ACM, 2011, pp. 141–154.

[5] B. Gozick, K. P. Subbu, R. Dantu, and T. Maeshiro, "Magnetic maps for indoor navigation," *IEEE Trans. Instrum. Meas.*, vol. 60, no. 12, pp. 3883–3891, 2011.

[6] B. Li, T. Gallagher, A. G. Dempster, and C. Rizos, "How feasible is the use of magnetic field alone for indoor positioning?" in *Int. Conf. on Indoor Positioning and Indoor Navigation*. IEEE, 2012, pp. 1–9.

[7] K. P. Subbu, B. Gozick, and R. Dantu, "Indoor localization through dynamic time warping," in *IEEE International Conference on Systems, Man, and Cybernetics*. IEEE, 2011, pp. 1639–1644.

[8] ——, "Locateme: Magnetic-fields-based indoor localization using smartphones," *ACM Trans. Intell. Syst. Technol.*, vol. 4, no. 4, p. 73, 2013.

[9] J. Haverinen and A. Kemppainen, "Global indoor self-localization based on the ambient magnetic field," *Robot. Auton. Syst.*, vol. 57, no. 10, pp. 1028–1035, 2009.

[10] Y. Shu, K. G. Shin, T. He, and J. Chen, "Last-mile navigation using smartphones," in *Annual International Conference on Mobile Computing and Networking*. ACM, 2015, pp. 512–524.

[11] M. Frassl, M. Angermann, M. Lichtenstern, P. Robertson, B. J. Julian, and M. Doniec, "Magnetic maps of indoor environments for precise localization of legged and non-legged locomotion," in *Proc. IEEE/RSJ Int. Conf. Intell. Robots Syst.* IEEE, 2013, pp. 913–920.

[12] N. Akai and K. Ozaki, "Gaussian processes for magnetic map-based localization in large-scale indoor environments," in *Proc. IEEE/RSJ Int. Conf. Intell. Robots Syst.* IEEE, 2015, pp. 4459–4464.

[13] Y. Shu, C. Bo, G. Shen, C. Zhao, and F. Zhao, "Magicol: Indoor localization using pervasive magnetic field and opportunistic wifi sensing," *IEEE J. Select. Areas Commun.*, vol. 33, no. 7, pp. 1443–1457, 2015.

[14] I. Vallivaara, J. Haverinen, A. Kemppainen, and J. Röning, "Simultaneous localization and mapping using ambient magnetic field," in *IEEE Conference on Multisensor Fusion and Integration for Intelligent Systems*. IEEE, 2010, pp. 14–19.

[15] P. Robertson, M. Frassl, M. Angermann, M. Doniec, B. J. Julian, M. Garcia Puyol, M. Khider, M. Lichtenstern, and L. Bruno, "Simultaneous localization and mapping for pedestrians using distortions of the local magnetic field intensity in large indoor environments," in *Int. Conf. on Indoor Positioning and Indoor Navigation*. IEEE, 2013, pp. 1–10.

[16] J. Jung, T. Oh, and H. Myung, "Magnetic field constraints and sequence-based matching for indoor pose graph SLAM," *Robot. Auton. Syst.*, vol. 70, pp. 92–105, 2015.

[17] C. Gao and R. Harle, "Sequence-based magnetic loop closures for automated signal surveying," in *Int. Conf. on Indoor Positioning and Indoor Navigation*. IEEE, 2015, pp. 1–12.

[18] S. Beauregard and H. Haas, "Pedestrian dead reckoning: A basis for personal positioning," in *Workshop on Positioning, Navigation and Communication*, 2006, pp. 27–35.

[19] M. Müller, "Dynamic time warping," *Information retrieval for music and motion*, pp. 69–84, 2007.

[20] N. Sünderhauf and P. Protzel, "Switchable constraints for robust pose graph SLAM," in *Proc. IEEE/RSJ Int. Conf. Intell. Robots Syst.* IEEE, 2012, pp. 1879–1884.

[21] A. Solin, M. Kok, N. Wahlström, T. B. Schön, and S. Särkkä, "Modeling and interpolation of the ambient magnetic field by gaussian processes," *arXiv preprint arXiv:1509.04634*, 2015.

[22] Google, "Google project tango," https://www.google.com/atap/project-tango/, 2016, [Online; accessed 20-Febrary-2016].

[23] K. H. Brodersen, C. S. Ong, K. E. Stephan, and J. M. Buhmann, "The binormal assumption on precision-recall curves," in *International Conference on Pattern Recognition*. IEEE, 2010, pp. 4263–4266.